

CHAPTER 78

RIP-CURRENT AND COASTAL TOPOGRAPHY

Mikio Hino

Professor, Department of Civil Engineering,
Tokyo Institute of Technology,
O-okayama, Meguro-ku, Tokyo, 152,
JAPAN

SUMMARY

At the 1974 Conference on Coastal Engineering (Copenhagen), the writer proposed a new theory on the mechanism of generation of rip-current and cuspidal coast that the alongshore homogeneous structure of wave field and movable sedimental bottom (that is two-dimensional wave setup and bottom topography) is unstable to a small perturbation, the motive force of instability being the radiation stresses caused by incident wave.

In this paper, based on the response concept and the mathematics already presented at the previous conference some improvements in solving the fundamental equations are attempted, since the direct solution of the full system of basic equations did not necessarily result in the sufficient conclusion.

The response of water-wave system to an infinitesimal perturbation in bottom boundary is quick enough compared with that of sediment system to a change occurring in water-wave system. Consequently, the water system is treated as quasi-stationary. By solving the equation of mass conservation of sediment transport under the prescribed boundary conditions, the preferred wavelength of rip-current as well as the profiles of velocity distribution and the bottom perturbation have been determined as an *eigenvalue* problem.

INTRODUCTION

Recently, various theories have been proposed on the mechanism of rip-current generation. These theories may be grouped into three categories; The forced formation theory, the variational principle of the energy dissipation and the instability or eigenvalue theory.

Bowen and Inman's theory published in 1969 is based on the forced mechanism caused by standing edge waves which induce the spatially periodic distribution of radiation stress.

On the other hand, the writer (Hino 1972) has proposed a hydrodynamic instability mechanism. The writer does not necessarily deny the mechanism proposed by Bowen & Inman. However, there may be a possibility of another mechanism for generation of rip-current system.

In 1971, the writer was staying about a month at the Louisiana State University where the writer and Dr. Sonu who is now at Tetra Tech, frequently discussed on this problem. Dr. Sonu considered that the bottom material would change to sinusoidal forms by the action of alongshore current, as if sandbars on river bed are formed by the unidirectional flow. While, the writer asserted on the instability of uniform wave setup.

ESSENCE OF THE PRESENT THEORY

The basic idea of the writer's theory is as follows;

(a) If waves are incident on a straight coast, and if the water depth is uniform along the shore, the uniform wave setup along it should be formed, caused by the radiation stress of incident waves.

Such a uniformly long wave setup may be unstable to an infinitesimal disturbance, as if a slender elastic cylinder compressed axially becomes buckled when a critical compressive stress is exceeded. This is the *buckling analogy*.

In other words, the wave system itself on a rigid plane bottom may be unstable to form the periodic rip-current. However, in real situations, the rip current is accompanied by the corresponding periodic perturbations in the bottom topography.

As has been indicated in the previous paper, the direct solution of the full system of equations yields the two types of instability; one with the high increase rate and the rapid translation velocity along the shore is called the "*fluid mode*", while the other with the slow rate of increase and the low convection velocity is terminated the "*bottom mode*". Except for the normal wave incidence or the standing wave case caused by positive and negative progressive waves, the fluid mode could not manifest itself because of the too rapid alongshore translation for the perturbation to grow into appreciable intensity.

(b) In solving for bottom mode the basic equations, a physical interpretation of the phenomenon concerned will be introduced. One important way of analysis of the modern fluid dynamics is to attack complicated problems not necessarily purely mathematically but to solve them after the simplification of original equations through the physical interpretation of the basic equations. This attitude has been established by L. Prandtl when he proposed the concept of boundary layer in 1904.

Turning to our problem, the response of water-wave system is quick enough to the deformation of bottom boundary, while the bottom materials respond very much slowly to the change in the water-wave system. Therefore, the state of fluid system may be considered to be quasi-stationary. This is the *concept of response time* (Hino 1974). This idea has already been presented and applied in the writer's first paper (Hino and Hayashi 1972).

(c) Consequently, the flow field for an arbitrary bottom profile is solved from the continuity and momentum equations which include the radiation stress terms introduced by Longuet-Higgins and Stewart (1964). The resulting solutions of velocity components and the water surface elevation still contain the undetermined parameters which describe the bottom profile.

(d) Finally, the above solutions are substituted into the balance equation of bottom material transport. The problem is thus reduced to the *eigenvalue problem*. The rate of increase in the bottom perturbation is determined by the real part of eigenvalues dependent on the alongshore wavenumber of perturbation. On the other hand, the imaginary part of the eigenvalue predicts the propagation velocity of bottom perturbation, that is sand bars.

The components of an eigen-vector determine the unknown coefficients to describe the resulting perturbation in bed profile and thus velocity distribution.

In this way, we can determine not only the predominant spacing of rip-current but also the resulting bottom shape, the velocity field and the water surface elevation.

The idea of the response concept and a simplified mathematical treatment have already been presented at the previous Copenhagen conference.

THEORY

(a) Basic Equations

The basic equations are the same as the previous paper ;

[Equations of motion]

$$\begin{aligned} \frac{\partial [\rho(h+\eta)u]}{\partial t} + \frac{\partial [\rho(h+\eta)u^2]}{\partial x} + \frac{\partial [\rho(h+\eta)uv]}{\partial y} + \frac{\partial S_{xx}}{\partial x} + \frac{\partial S_{xy}}{\partial y} \\ = -\rho g(h+\eta) \frac{\partial \eta}{\partial x} - \rho \zeta u \end{aligned} \quad (1)$$

$$\begin{aligned} \frac{\partial [\rho(h+\eta)v]}{\partial t} + \frac{\partial [\rho(h+\eta)uv]}{\partial x} + \frac{\partial [\rho(h+\eta)v^2]}{\partial y} + \frac{\partial S_{xy}}{\partial x} + \frac{\partial S_{yy}}{\partial y} \\ = -\rho g(h+\eta) \frac{\partial \eta}{\partial y} - \rho \zeta v \end{aligned} \quad (2)$$

[Continuity equation]

$$\frac{\partial (h+\eta)}{\partial t} + \frac{\partial [u(h+\eta)]}{\partial x} + \frac{\partial [v(h+\eta)]}{\partial y} = 0 \quad (3)$$

[Radiation stress relationship]

$$\begin{aligned} S_{xx} &= \frac{3E}{2} - Ec^2 \left(\frac{\sin\theta}{c}\right)^2 \\ S_{yy} &= \frac{E}{2} + Ec^2 \left(\frac{\sin\theta}{c}\right)^2 \\ S_{xy} &= Ec \cos\theta \left(\frac{\sin\theta}{c}\right) \end{aligned} \quad (4)$$

$$E = (\rho g \gamma^2 / 8) (h + \eta)^2 \quad (5)$$

$$c = \{g(h + \eta)\}^{1/2} \quad (6)$$

where $\tilde{\gamma}=1$ inside of breaker zone and zero outside of it.
[Balance equation of bottom material transport]

$$\frac{\partial h}{\partial t} = \frac{\partial(C_s u)}{\partial x} + \frac{\partial(C_s v)}{\partial y} \quad (7)$$

In the above equations, the coordinate system is chosen as shown in Fig. 1 ; u, v mean the velocity components in the x - and y -direction, respectively ; η and h are the mean water-level elevation above still water surface and the depth of bottom, respectively ; S_{xx}, S_{xy} , and S_{yy} represent the radiation stress tensor components ; c is the wave velocity, E the wave energy per unit area, \tilde{C} and C_s are the coefficients of bottom friction and bottom material transport, respectively.

(b) Perturbation Equations

Variables are expressed as sum of equilibrium states ($0, V_0, \eta_0$, and h_0) and small perturbations (u, v, η and h)

$$\begin{aligned} u(x, y, t) &\rightarrow u(x, y, t) \\ v(x, y, t) &\rightarrow V_0(x) + v(x, y, t) \\ \eta(x, y, t) &\rightarrow \eta_0(x) + \eta(x, y, t) \\ h(x, y, t) &\rightarrow h_0(x) + h(x, y, t) \end{aligned} \quad (8)$$

Furthermore, variables are nondimensionalized by L_b (the distance from shore to breaker) and $\sqrt{gL_b}$,

$$\begin{aligned} u/\sqrt{gL_b} &\rightarrow u, \quad v/\sqrt{gL_b} \rightarrow v, \quad V_o/\sqrt{gL_b} \rightarrow V_o \\ x/L_b &\rightarrow x, \quad y/L_b \rightarrow y, \quad h_o/L_b \rightarrow h_o \\ t\sqrt{g/L_b} &\rightarrow t, \quad c/\sqrt{gL_b} \rightarrow c, \quad C_s/L_b \rightarrow C_s \end{aligned} \quad (9)$$

Substituting eq.(8) into eqs.(1) through (7) and linearizing, a set of the linear partial equations are derived,

$$\begin{aligned} \frac{\partial w_i}{\partial t} + A_{i1}(x)\frac{\partial u}{\partial x} + A_{i2}(x)\frac{\partial u}{\partial y} + a_i(x)u \\ + B_{i1}(x)\frac{\partial v}{\partial x} + B_{i2}(x)\frac{\partial v}{\partial y} + b_i(x)v \\ + C_{i1}(x)\frac{\partial \eta}{\partial x} + C_{i2}(x)\frac{\partial \eta}{\partial y} + c_i(x)\eta \\ + D_{i1}(x)\frac{\partial h}{\partial x} + D_{i2}(x)\frac{\partial h}{\partial y} + d_i(x)h = 0 \end{aligned} \quad (10)$$

(i=1,2 and 3)

$$\frac{\partial h}{\partial t} = \frac{\partial C_s u}{\partial x} + \frac{\partial C_s u}{\partial y} \quad (11)$$

where $w_1=u$, $w_2=v$ and $w_3=\eta$, and V_o and $d\eta_o/dx$ which are given as the zero-th order approximation of the perturbation mean the alongshore current velocity and the gradient of wave-setup, respectively ;

$$\begin{aligned} V_o(x) = -\frac{5\gamma^2}{16C_d}(\cos\theta \cdot \sin\theta_b \cdot \sqrt{h_{ob} + \eta_{ob}}) \\ \cdot \frac{h_o + \eta_o}{h_{ob} + \eta_{ob}} \frac{d(h_o + \eta_o)}{dx} \end{aligned} \quad (12)$$

$$\frac{d\eta_o}{dx} = -\left(\frac{3\gamma^2}{8}\right) \frac{\cos^2\theta}{[1+(3\gamma^2/8)\cos^2\theta]} \cdot \frac{dh_o}{dx} \quad (13)$$

Coefficients A_{ij} , B_{ij} etc. are generally functions of x (For details, reference should be made to a paper (Hino 1975).).

(c) Quasi-steady Solution of Water System to Bottom Perturbation

The perturbation in depth profile $h(x,y)$ is expressed by the orthogonal Hermite functions as eq.(14),

$$h(x,y) = \delta \sum_n \mu_n / (\sqrt{(n-1)!}) \cdot H_{n-1}(x) e^{-x^2/4} e^{iky} \quad (14)$$

where δ expresses a parameter of amplitude, H_n is the Hermite function of n -th order and the expansion coefficients μ_n are unknown arbitrary constants to be determined later as a result of the eigenvalue problem.

The solution of fluid system (the velocity components u and v , and the mean surface elevation η) is assumed to be expanded also by the Hermite series as

$$\begin{aligned} u(x,y;t) &= \sum \frac{\alpha_{2n'}}{\sqrt{(2n'-1)!}} H_{2n'-1}(x) e^{-x^2/4} e^{iky} \\ v(x,y;t) &= \sum \frac{\beta_n}{\sqrt{(n-1)!}} H_{n-1}(x) e^{-x^2/4} e^{iky} \\ \eta(x,y;t) &= \sum \frac{\gamma_n}{\sqrt{(n-1)!}} H_{n-1}(x) e^{-x^2/4} e^{iky} \end{aligned} \quad (15)$$

where the boundary condition that u equals zero at $x=0$ is considered by using only the odd-order Hermite functions; and the boundary conditions that at infinite x variables approach zero by the property of Hermite

functions ($H_n(x)e^{-x^2/4} \rightarrow 0$, when $x \rightarrow \infty$).

Substitution of eqs.(14) and (15) into eqs.(10), and applying the Galerkin method, i.e. integrating them between $(0, \infty)$ after multiplication of both hand side by $H_{m'-1}(x)e^{-x^2/4}/\sqrt{(m'-1)!}$ and putting the residue equal to zero, a set of simultaneous equations for coefficients vector $X = [\alpha_2, \alpha_4, \dots, \beta_1, \beta_2, \dots, \gamma_1, \gamma_2, \dots]^T$ is obtained as a function of $h(x,y)$ or coefficients μ_n ,

$$\begin{aligned} X &= -\delta(A^{-1}B)\mu \\ &= \delta D\mu \end{aligned} \quad (16)$$

$$\begin{aligned} X &= [\alpha_2, \alpha_4, \dots, \alpha_{N'}, \beta_1, \beta_2, \dots, \beta_N, \gamma_1, \gamma_2, \dots, \gamma_N]^T \\ & \quad ((N'+2N)+1 \text{ matrix}) \end{aligned} \quad (17)$$

$$A = \begin{bmatrix} I^{(1)} & J^{(1)} & K^{(1)} \\ I^{(2)} & J^{(2)} & K^{(2)} \\ I^{(3)} & J^{(3)} & K^{(3)} \end{bmatrix} \begin{matrix} ((N'+2N) \\ \times (N'+2N) \text{ matrix}) \end{matrix} \quad (18)$$

$$B = \begin{bmatrix} L^{(1)} \\ L^{(2)} \\ L^{(3)} \end{bmatrix} \quad (19)$$

$$D = \begin{bmatrix} a'_1 \\ \vdots \\ a'_N \\ b_1 \\ \vdots \\ b_N \\ c_1 \\ \vdots \\ c_N \end{bmatrix} \quad (20)$$

$$\begin{aligned} a'_k &= [a_{k1}, a_{k2}, \dots, a_{kN}] \\ b_k &= [b_{k1}, b_{k2}, \dots, b_{kN}] \\ c_k &= [c_{k1}, c_{k2}, \dots, c_{kN}] \end{aligned} \quad (21)$$

$$\mu = [\mu_1, \mu_2, \dots, \mu_N]^T \quad (22)$$

The elements of submatrices $I^{(i)}$, $J^{(i)}$, $K^{(i)}$ and $L^{(i)}$ are given in terms of coefficients A_{ij} , B_{ij} , \dots , a_i , b_i and so on (Hino 1975).

Matrix D ($(N'+2N) \times N$ matrix) which can be decomposed into row vectors represents the contribution rate of bottom perturbation component $H_{n-1}(x)e^{-x^2/4}$ to velocity and mean surface elevation, u , v and η .

(c) Stability of Bottom Perturbation (Eigenvalue Problem of Bottom Mode Instability)

From the response concept, the amplitude factor δ of eq.(14) is assumed now a slowly varying function of time. Substitution of equations of u , v , η and h where the unknowns are the coefficient vector μ and the amplitude factor δ into eq.(11) yields

$$\begin{aligned} \dot{\delta}(t) & \sum_{n=1}^{\infty} \frac{H_n}{\sqrt{(n-1)!}} H_{n-1}(x) e^{-x^2/4} e^{iky} \\ & = \delta(t) C_s \left[\sum_{n=1}^{\infty} a_n \mu \{ H'_{n-1}(x) - \frac{x}{2} H_{n-1}(x) \} \right. \\ & \left. + (ik) \sum_{n=1}^{\infty} b_n \mu H_{n-1}(x) \right] e^{-x^2/4} e^{iky} \end{aligned} \quad (23)$$

Again applying the Galerkin technique, the following equation is obtained,

$$T\mu = p\mu \quad (24)$$

where p is the exponential growth rate

$$p = (d\delta/dt)/(C_s \delta) \quad (25)$$

and matrix T is composed of coefficients in matrix D (eqs.(43) through (47) in Hino, 1975).

Eq.(24) poses an eigenvalue problem for matrix T , the unknowns p and μ being eigenvalues and eigenvectors, respectively. These are solved numerically by a digital computer HITAC 8700/8400 of Computer Center, Tokyo Institute of Technology.

Two non-dimensional parameters, χ and ψ , are defined from factors affecting the phenomenon,

$$\begin{aligned} \chi & = s(\sin \theta/c)^2 \\ & = (h_b/L_b) \cdot (\sin \theta_b / \sqrt{h_b/L_b})^2 \\ & = \sin^2 \theta_b \end{aligned} \quad (26)$$

$$\begin{aligned} \psi & = s^2(\sin \theta_b/c) \\ & = (h_b/L_b)^{3/2} \sin \theta_b . \end{aligned} \quad (27)$$

RESULTS

(a) Instability diagram:

Fig. 2 shows some examples from the instability diagrams. The exponential growth rates (the maximum values of the real part of eigenvalues), $(Pr)_{\max}$, are plotted against the alongshore wavenumber k of perturbation for a selected combination of bottom slope $h_b = sL_b$ (L_b : distance to breaker zone). In these graphs, the parameter θ expresses the incident angle of waves.

It is shown that the perturbation in bottom configuration and consequently in wave field is most unstable to a certain wave number k_* of alongshore periodicity. Except for the normal incidence, $\theta=0$, the amplification rates become maximum at the nondimensional alongshore wave number of about $k=1.5$ or at the wave length of about 4 times the distance from shore to breaker.

Fig. 3 shows the relation between the most preferred alongshore wavenumber (nondimensional) k_* , the angle of incidence θ and the slope of the initial bottom s . As the bottom slope becomes steep, the preferred nondimensional spacing of rip current ($L_R = 2\pi/k_*$) increases. However, since the distance of breaker from shore also reduces, the real spacing of rip current (L_R)

$$\begin{aligned} L_R &= (2\pi/k_*) L_b \\ &= 2\pi h_b / s k_* \end{aligned} \quad (28)$$

(where h_b is the breaker depth) is estimated generally to become shortened.

(b) Propagation celerity of sandbars:

Moreover, it should be added that the present theory gives the celerity of alongshore translation of bottom perturbation as

$$C_* = p_i C_S / k \quad (29)$$

where p_i represents an imaginary part of the eigenvalue. Fig. 4 is a plot of the propagation velocity of sand bars.

(c) Rip-current and rip-channel:

By substituting the eigenvectors μ which determine the coefficients of perturbed bottom profile in eq. (24), into the series expression (eqs. (14) and (10)) of variables u , v , ζ and h , we are able to obtain the profiles of sand bars and the velocity fields.

Fig. 5 is the cross-sectional profile of a sand bar at various position along the shore. From this graph, a conclusion is derived that sand bars seem to progress onshore when observed at a cross-section perpendicular to the shore, although in reality they are propagated alongshore.

In Fig 6, the upper solid line gives the velocity of offshore current u , that is the rudimentary rip-current. The strength of velocity is the highest at the breaker zone. The lower thin solid curve is the change of bottom profile. This is the so-called rip-channel. The bottom is eroded inside and near the breaker zone, while sand materials are deposited offshore.

These results of theoretical analysis (Figs. 5 and 6) agree well with observed facts.

(d) Effect of initial bottom shape:

The initial bottom profiles are assumed to be represented by

$$h_0(x,y) \propto x^n \quad (30)$$

The upward convex bottom and the upward concave bottom are represented by $n > 1$ and $0 < n < 1$, respectively. Fig. 7 shows the instability diagrams for both cases, indicating that the upward convex shallow bottom is apt to change into rip current system.

(e) Relative importance of wave-setup, alongshore current and bottom friction:

The writer is interested in the relative importance of various intrinsic factors, such as those,

- (i) the wave setup which is caused by the radiation stress,
- (ii) the intensity of alongshore current which is also driven by the radiation stress,
- (iii) the friction factor which influences the intensity of alongshore current.

Since these factors are closely inter-connected each other, it is difficult separated them experimentally. However, in the theoretical analysis, it is possible to change artificially, for instance, the intensity of alongshore current alone, keeping the radiation stress or wave setup unchanged.

Fig. 8 (b) is the instability diagram when the radiation stress parameter γ is varied, keeping the alongshore current (lsc) unchanged. As the intensity of radiation stress is decreased the amplification rate of perturbation decreases. In reality, as the intensity of radiation stress is decreased, the alongshore current is also reduced. The left hand side figure (Fig. 8 (a)) shows the theoretical result for this case ($lsc = \text{real}$).

Fig. 8 (c) gives the instability diagram for a hypothetical case of no alongshore current ($lsc = 0$) even if there is the wave setup, when waves are incident obliquely. In this hypothetical case, the infinitesimal perturbation is also unstable; however there exist no predominant preferred wave number. The tendency is similar to the case of normal wave incidence ($\theta = 0$).

Fig. 9 (a) and (b) summarizes the results on the relationship between the radiation stress intensity and the preferred wavenumber of rip-current spacing ($\gamma \sim k_*$) and the exponential growth rate ($\gamma \sim \rho_*$), respectively.

One the other hand, Fig.10 examines the effects of the bottom friction, keeping the wave setup unchanged ; i.e. $\gamma=1$. Fig.10 (a) is the result for real case, Fig.10 (b) and (c) being the results for hypothetical cases of unchanged and no-alongshore current, respectively.

Fig. 11 (a) and (b) summarizes these results.

From these analytical computation, the following conclusion may be deduced ;

- (i) The main trigger of rip-current generation is the wave-setup caused by the radiation stress, rather than the alongshore current.
- (ii) The spacing of rip-current is dependent on the strength of alongshore current. If there were no alongshore current, there occurs no predominate wavenumber. As the intensity of alongshore current is increased, or the bottom friction is decreased, the preferred wavenumber of rip-current decreases. In other words, the spacing of rip-current becomes longer.
- (iii) When there is no wave-setup, the rip-current would not be formed, even if there were the alongshore current (c.f. especially, Fig. 8 (b) where the intensity of the alongshore current is as strong as for the case of real case caused by the radiation stress).

REFERENCES

- 1) Bowen, A.J. (1969): J. Geophy. Res., Vol.74, No.23, pp.5467-5478.
- 2) Hino, M. and Hayashi, N. (1972): Coastal Engineering in Japan, Vol. 16, pp.55-60, (in English).
- 3) Hino, M. (1974): Proc. 14th International Conference on Coastal Eng., Copenhagen, June.
- 4) Hino, M. (1975): Proc. Japan Soc. Civil Eng., No.237, pp.87-98.
- 5) Longuet-Higgins, M.S. and Stewart, R.W. (1964): Deep-Sea Res., Vol. 11, pp.529-562.
- 6) Sonu, C.J. (1972): J. Geophy. Res., Vol.77, No.18, pp.3232-3247, June.

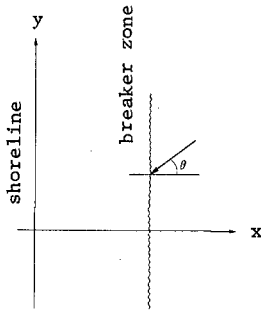


Fig. 1 ; Coordination, x:offshore direction, y:alongshore direction, θ :incidence angle of wave.

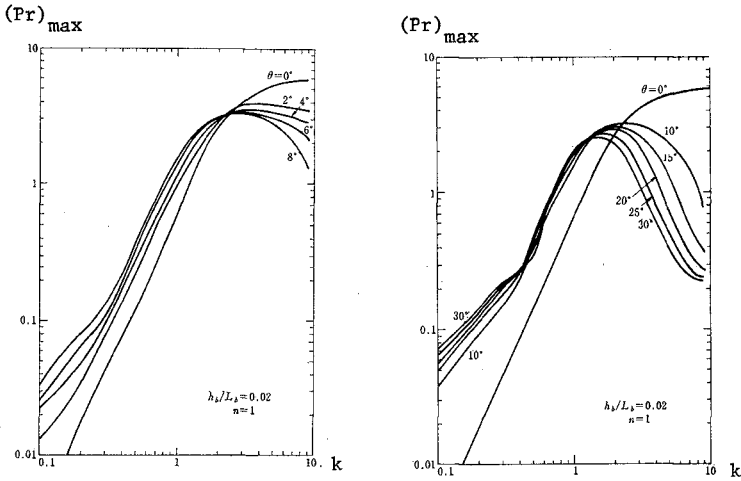


Fig. 2 ; Longshore wave number and the maximum exponential growth rate.

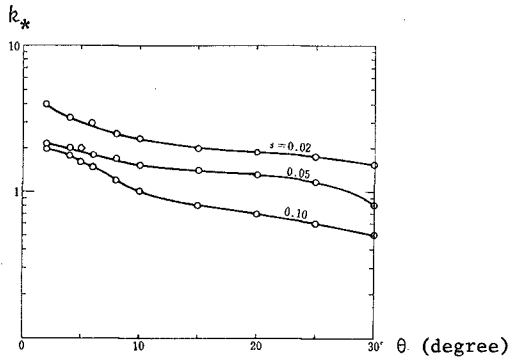


Fig. 3 ; Relationship between the most preferred longshore wave number k_* , the angle of wave incidence θ_b and the bottom slope s .

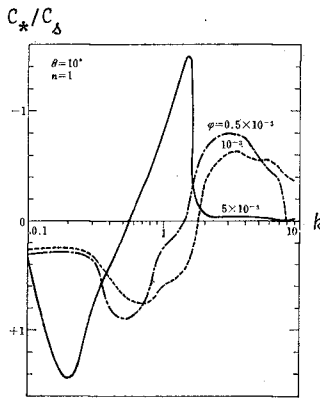


Fig. 4 ; Longshore wave number and translation celerity of sand-bar.

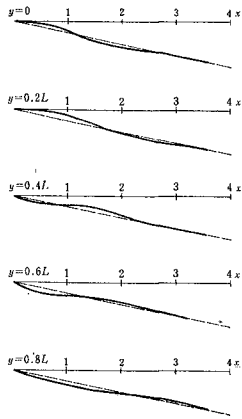


Fig. 5 ; Cross-sectional profiles of sand-bar at various position of y ,

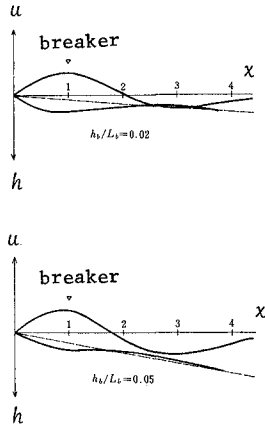


Fig. 6 ; Velocity distribution of offshore current at the rudimentary rip-current $u(x, y_0)$ and the depth variation of bottom (the so-called rip-channel) $h(x, y_0)$.

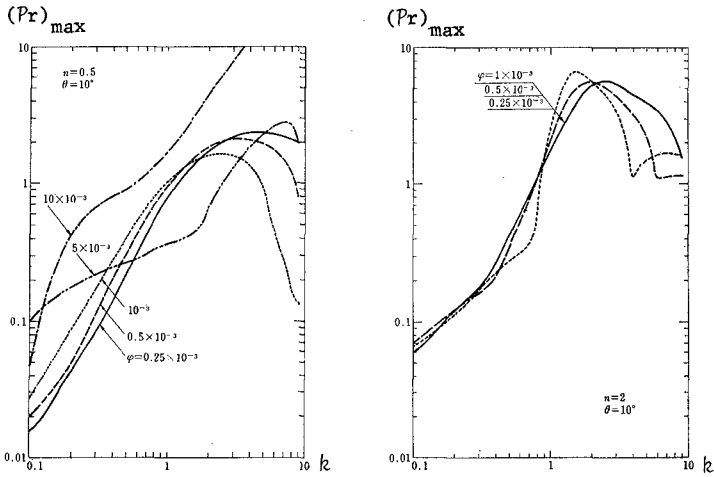


Fig. 7 ; Effects of the initial bottom shape ($h_0(x) \propto x^n$) on the relationship k and $(Pr)_{max}$, (a) for a concave bottom of $n=0.5$ and (b) for a convex bottom of $n=2$.

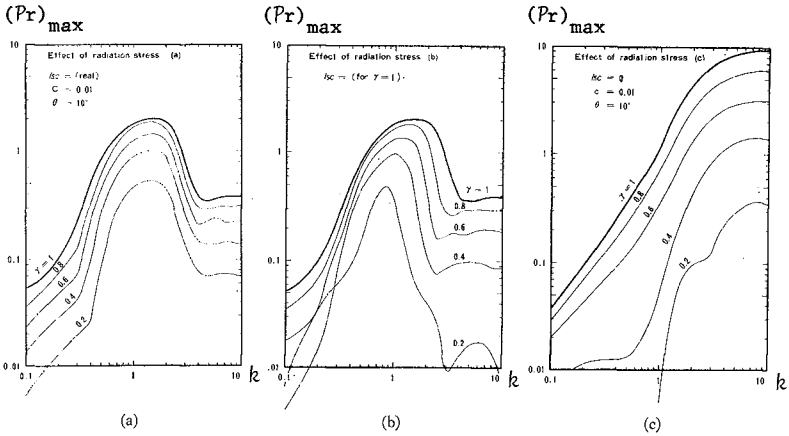


Fig. 8 ; Effect of the radiation stress intensity (γ) on the exponential growth rate $(Pr)_{max}$ and longshore wave-number k .

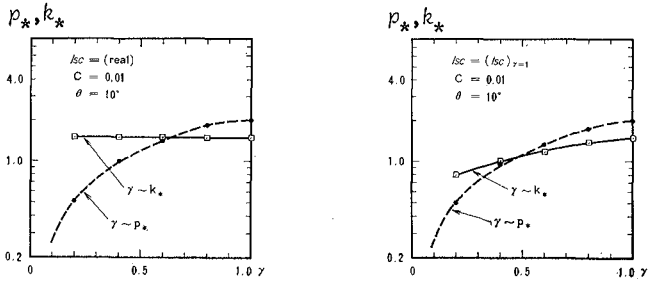


Fig. 9 ; Effect of the intensity of radiation stress γ on the most preferred longshore wave-number k_* and the corresponding exponential growth rate p_* .

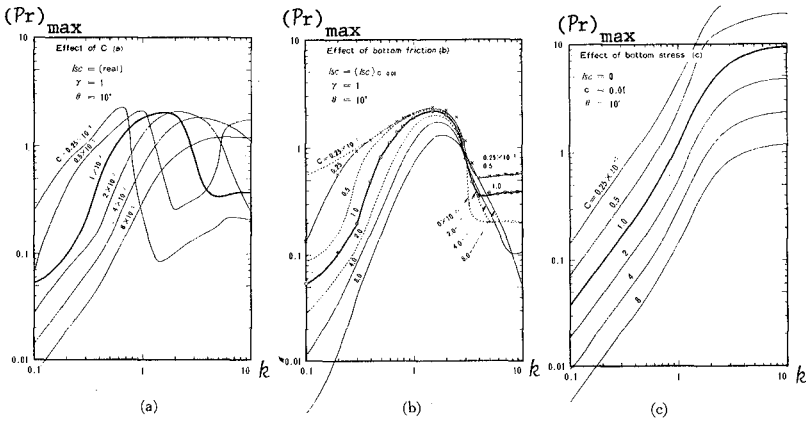


Fig.10 ; Effect of the bottom friction on the instability diagram.

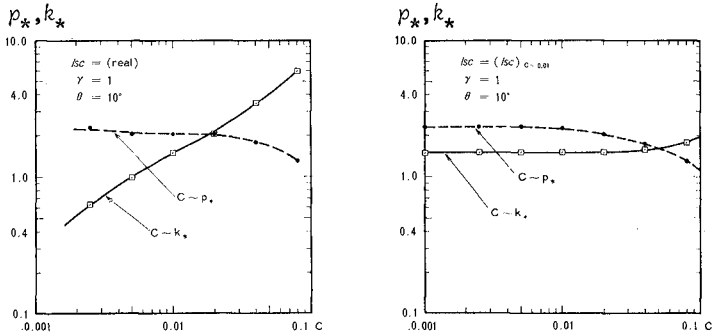


Fig.11 ; Effect of the bottom friction on the most preferred longshore wave number k_* and the exponential growth rate p_* .